



# Light-excited photoelectrons coupled with bio-photocatalysis enhanced the degradation efficiency of oxytetracycline

Rui Ding <sup>a, b</sup>, Weifu Yan <sup>a</sup>, Yan Wu <sup>b, c</sup>, Yong Xiao <sup>a</sup>, Haiyin Gang <sup>a</sup>, Shuhua Wang <sup>a, b</sup>, Lixiang Chen <sup>a, b</sup>, Feng Zhao <sup>a, \*</sup>

<sup>a</sup> Key Laboratory of Urban Pollutant Conversion, Institute of Urban Environment, Chinese Academy of Sciences, Xiamen, 361021, China

<sup>b</sup> University of Chinese Academy of Sciences, Beijing, 100049, China

<sup>c</sup> Institute of Urban Environment, Chinese Academy of Sciences, Xiamen, 361021, China

## ARTICLE INFO

### Article history:

Received 16 March 2018

Received in revised form

9 June 2018

Accepted 28 June 2018

Available online 29 June 2018

### Keywords:

Photoelectrons

Biodegradation

Photocatalytic degradation

Synergistic degradation

Oxytetracycline

## ABSTRACT

Intimately coupled photocatalysis and biodegradation (ICPB) is a novel wastewater treatment technique that has potential applications in refractory degradation. This paper reports a synergistic degradation protocol that allowing the transfer of photoelectrons between photocatalysts and microbes without supplementary electron donors or improving the loading rate of the photocatalysts. As a result, a degradation rate of ~94% was sustained for 400 h in a perturbation setup with a hydraulic retention time of 4.0 h. We achieved the degradation of  $\beta$ -apo-oxytetracycline, a stable antimicrobial intermediate compound (half-life of 270 d in soil interstitial water), within 10 min, and no accumulation was observed. Moreover, the required loading rate of the photocatalyst was dramatically reduced to 18.3% compared to previous reports which mentioned much higher rates. The results of our study provided a new strategy to improve the degradation efficiency of oxytetracycline and give new insight into the degradation mechanism of the bio-photocatalytic degradation system.

© 2018 Elsevier Ltd. All rights reserved.

## 1. Introduction

Antibiotics are manufactured and prescribed to control bacterial infections in humans and agriculture. An estimated 200 000 tons of antibiotics are produced per year, tetracyclines being the most commonly used (Vaz et al., 2015). Oxytetracycline, one of the most widespread prophylactic antibiotics used in personal care products for its broad-spectrum activity and low cost, has been detected in soil, water, and even food products, in concentrations ranging from ppb to ppm (Ashfaq et al., 2017; Li et al., 2004). The polyaromatic ring-structure of oxytetracycline confers its chemical stability and relatively long half-life in the environment, which promotes the terrifying for antibiotics pollution (Yan et al., 2018).

A number of chemical oxidation methods (e.g., photolysis (Zhao et al., 2013), photocatalysis (Chen et al., 2016) and photo-Fenton oxidation (Pereira et al., 2014)) have been applied to study the removal of oxytetracycline in water. Although these processes are fast and robust, full mineralization is economically prohibitive and

practically difficult (Li et al., 2011). To overcome these drawbacks, the intimately coupled photocatalysis and biodegradation (ICPB) process emerged and had been used widely (Ding and Zhao, 2017; Marsolek et al., 2008; Rittmann, 2017). In this process, photocatalysts and biofilms were coated onto the same carrier, wherein, the photocatalytic performance occurred on the outer surface, while biodegradation took place inside (Li et al., 2011; Marsolek et al., 2008; Wen et al., 2012). The biofilm was well sheltered from toxicants and oxidants due to the protection of the carrier. As the combined degradation process was repeated, compounds were effectively degraded.

Significant efforts have been made to promote the mineralization ability of the combined system, including the following effective strategies: building carriers that are less susceptible to deterioration (Wen et al., 2012), fabricating new types of photocatalysts (Zhang et al., 2016), increasing the loading rate of the photocatalyst to maintain photocatalytic efficiency (Li et al., 2012a), and providing extra electron donors to maintain a robust biofilm community (Xiong et al., 2018). So far, the combined degradation systems have been investigated for denitrification (Wen et al., 2012), dechlorination (Zhou et al., 2017), and degradation of dyes (Li et al., 2012b) and antibiotics (Xiong et al., 2017), revealing their

\* Corresponding author.

E-mail address: [fzhao@iue.ac.cn](mailto:fzhao@iue.ac.cn) (F. Zhao).

potential for applications in practical wastewater treatment.

In this study, we provided a simple protocol to modify the ICPB process and enhance the degradation efficiency of oxytetracycline. As shown in Scheme 1, light excitation of photoelectrons coupled with bio-photocatalysis was developed as a synergistic degradation method. During the degradation process, a carrier with higher porosity than those utilized in previous works was used. Instead of protecting biofilms by placing them inside carriers, the photocatalysts and microorganisms were coated full of the carriers. The transfer of the light excited photoelectrons between photocatalysts and microorganisms occurred under visible light irradiation. Thus, photocatalytic degradation, microbial metabolic degradation, and the transfer of photoelectrons between photocatalysts and microbes as an assisted degradation method occurred simultaneously.

Many studies have illustrated the sterilization effect of photocatalysis. However, it has been demonstrated that microorganisms could use light excited electrons through the photocatalysis of semiconductors to stimulate growth, sustain cellular metabolism, regulate community structure, and contribute to environmental remediation (Duan et al., 2013; Lovley, 2011; Lu et al., 2012; Sakimoto et al., 2016). In addition, although microbes should have been protected inside the carriers in the previous works, few bacteria were still found on the outer surfaces of carriers (Li et al., 2012a; Zhou et al., 2015), indicating the survival of microbes and their resistance to negative influences. To demonstrate the feasibility of this protocol, the degradation efficiency, evolution of byproducts, the stability of degradation performance for oxytetracycline, and bio-transformation during the process were evaluated. The results confirmed that stimulating the transfer of photoelectrons between photocatalysts and microbes was a useful method to enhance the degradation efficiency of the bio-photocatalysis process.

## 2. Materials and methods

### 2.1. Chemicals and reagents

The oxytetracycline (purity of 95.6%) and  $\beta$ -apo-oxytetracycline (purity of 95.6%) standards were sourced from Dr. Ehrenstorfer GmbH (Augsburg, Germany). The methanol, acetonitrile, and formic acid used were of high-performance liquid chromatography (HPLC) grade and were purchased from Merck KGaA (Darmstadt, Germany). The other chemicals and reagents were of analytical grade and purchased from Sinopharm Group Co. Ltd. (Shanghai, China). Ultrapure water was used throughout the experiment.

### 2.2. Carrier and coating of the photocatalyst

The carrier used in this study was a commercially available polyurethane sponge cube (Ai' qin Environmental Technologies Co., Ltd., Jiangsu, China) (Fig. S1), with an average side length of  $3.0 \pm 0.1$  mm. According to the manufacturer, the carrier had a higher porosity (95%) than that of carriers used in previous works (Table S1) and a specific surface area of  $1.5 \text{ m}^2/\text{g}$ .

In this study, inexpensive and highly efficient belt-shaped one-dimensional oxygen-rich  $\text{Bi}_{12}\text{O}_{17}\text{Cl}_2$  was used as photocatalyst. We prepared  $\text{Bi}_{12}\text{O}_{17}\text{Cl}_2$  using a previously described method (Wang et al., 2017). The detailed preparation method and characterization of  $\text{Bi}_{12}\text{O}_{17}\text{Cl}_2$  (Fig. S2 and S3) were illustrated in the Supplementary Material. We used the following procedure for coating: 2.0 g  $\text{Bi}_{12}\text{O}_{17}\text{Cl}_2$  and 2.0 g uncoated carrier cubes were ultrasonically dispersed in 100.0 mL  $\text{C}_2\text{H}_5\text{OH}$  to obtain a homogeneous suspension. Subsequently, the above suspension was heated to  $80^\circ\text{C}$  under persistent magnetic stirring until all the liquid evaporated. To remove the unbounded  $\text{Bi}_{12}\text{O}_{17}\text{Cl}_2$ , the coated carrier cubes were ultrasonicated for 5 min. Finally, the coated carriers were dried, and the coating coverage on the carriers was determined to be 18.3%.

### 2.3. Microbe cultivation method

We collected swine wastewater effluent from a farm (Lesen, Xiamen, China). After diluting the wastewater using 100 mM phosphate buffer solution (PBS,  $\text{pH} = 7.0$ ), the supernatant was collected, and oxytetracycline was added as carbon source. Finally, 10.0 mg/L oxytetracycline was added during the acclimation of microbes for approximately one year to simulate the proliferation of functional microbial groups as it would occur in wastewaters containing a high concentration of oxytetracycline. Subsequently, the acclimated microbes were separated by centrifugation at 7500 rpm for 10 min. For cultivation, the  $\text{Bi}_{12}\text{O}_{17}\text{Cl}_2$ -coated carriers and collected microbes were mixed in a culture solution that contained 100 mM PBS, a nitrogen source, and sodium acetate (Table S2). Cultivation lasted for one week, and the supporting solution was refreshed every two days.

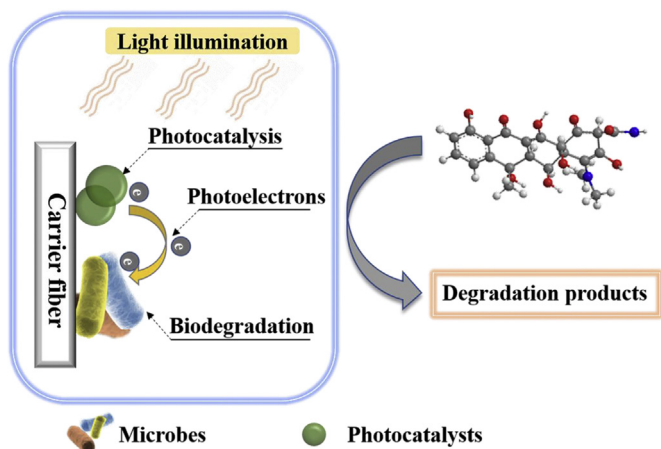
### 2.4. Degradation activity tests

The degradation activity was measured in static and perturbed systems. A 300 W tungsten halogen lamp (Philips, The Netherlands) with a wavelength range from 400 nm to 780 nm, equipped with a filter was used as visible light source. The light intensity was  $80 \text{ mW}/\text{cm}^2$ , which was close to the average value of the visible light spectrum of sunlight. Photocatalytic experiments were carried out at  $22 \pm 2^\circ\text{C}$  while using a circulating water system to prevent thermal catalytic effects.

The initial concentration of oxytetracycline for the degradation tests was 10.0 mg/L. For the static system, each experiment was conducted using a 150 mL beaker containing 75 mL of degradation liquid (Table S3). The concentration of  $\text{Bi}_{12}\text{O}_{17}\text{Cl}_2$  used was 1.0 mg/mL. A Shimadzu TOC-VWP analyzer was used to determine the total organic carbon (TOC). The synergistic degradation activities in the perturbed system were evaluated by mixing the degradation liquid (Table S3) with supplemental inorganic salt (10 mL/L), as shown in Table S4. The influent was supplied at a flow rate of 0.41 mL/min, which provided a hydraulic retention time (HRT) of 4.0 h. Both  $\text{Bi}_{12}\text{O}_{17}\text{Cl}_2$  and the microorganisms were coated on the carriers for photocatalytic degradation and biodegradation.

### 2.5. Analytical methods

The remnant oxytetracycline was analyzed using a Hitachi L-



Scheme 1. Degradation mechanisms of the modified carrier in ICPB.

2000 series HPLC instrument with UV detection at 278 nm. Each sample was centrifuged at  $10\,000 \times g$  for 15 min before testing. Oxytetracycline separation was achieved using an Agilent Zorbax Eclipse plus C18 column ( $4.8 \times 250$  mm, 5 mm). The optimized mobile phase consisted of 78% 0.014 M oxalic acid solution (phase A), 12% methanol (phase B), and 10% acetonitrile (phase C) at a flow rate of 1.0 mL/min. A 10.0  $\mu$ L sample was injected into the column, and the temperature of the column was 30 °C.

The exponential decay model  $C = C_0 e^{-kt}$  was used to calculate the kinetics transformation of oxytetracycline as previously described (Liang et al., 2013), where  $C$  (mg/L) represents the concentration of oxytetracycline at time  $t$  (h). The rate constant  $k$  (1/h) was obtained by using the Origin 8.0 software, and the half-life ( $t_{1/2}$ ) was calculated from the equation  $t_{1/2} = 0.693/k$ .

Separation and analysis of the byproducts were achieved using a liquid chromatography/orbitrap-mass spectrometry system (Thermo, USA) in full-scan positive-ion mode after desalination pretreatment through the hydrophilic-lipophilic balance (HLB) column. The mass spectrometer was operated in the 100–1000 mass-to-charge ( $m/z$ ) ratio range. Chromatographic separation of the byproducts was performed on an ACQUITY ultra performance liquid chromatography (UPLC) ethylene bridged hybrid (BEH) C18 Column (1.7  $\mu$ m,  $2.1 \times 100$  mm) with an injection volume of 5.0  $\mu$ L. A gradient of water containing 0.1% formic acid (phase A) and methanol containing 0.1% formic acid (phase B) was used to elute the analytes at 400.0  $\mu$ L/min and generated the following profile: B: 5.0% (0.0  $\rightarrow$  1.0 min), 5.0  $\rightarrow$  40.0% (1.0  $\rightarrow$  7.0 min), 40.0  $\rightarrow$  100.0% (7.0  $\rightarrow$  9.0 min), 100.0% (9.0  $\rightarrow$  13.0 min), 100.0  $\rightarrow$  5.0% (13.0  $\rightarrow$  13.1 min), 5.0% (13.1  $\rightarrow$  15.0 min).

## 2.6. Photo-electrochemical measurements

Photo-electrochemical tests were performed utilizing the three-electrode configuration using an electrochemical workstation (CHI660D, CH Instruments Inc., China). We used blank or modified stainless steel wire ( $1.0 \times 1.5$  cm) as working electrodes, a carbon rod as counter electrode, Ag/AgCl, KCl (sat'd) as reference electrode, and 100 mM PBS (pH = 7.0) as electrolyte. We obtained amperometric I-t curves and conducted photo-electrochemical impedance spectroscopy (EIS) analysis without bias. Linear sweep voltammograms were measured between 0.45 and 0.85 V. Moreover, we used a light density of 80 mW/cm<sup>2</sup> for each illuminated test.

## 2.7. Microbial community analysis

Bio-samples were collected to study the biotransformation that occurred during the removal of oxytetracycline from the synergetic system. The raw sample was coated onto the carriers before the test. The BP samples were microorganisms from the synergetic system after 400 h of degradation. DNA extraction was carried out using a FastDNA SPIN Kit for Soil (MP Biomedicals, USA). The extracted DNA samples were analyzed at Majorbio Bio-pharm Technology Co., Ltd (Shanghai, China). The selected bacterial primers were 338F (ACTCCTACGGGAGGCAGCAG) and 806G (GGACTACHVGGGTWTCTAAT). Polymerase chain reaction (PCR) amplification was performed using 4.0  $\mu$ L 5  $\times$  FastPfu buffer, 2.0  $\mu$ L deoxyribonucleotide triphosphate (dNTP) (2.5 mM), 0.8  $\mu$ L forward and reverse primers (5.0  $\mu$ M), respectively, 0.4  $\mu$ L FastPfu Polymerase, 0.2  $\mu$ L bovine serum albumin (BSA), and 10.0 ng template DNA. Finally, PCR-grade water was added to the mixture above to obtain a final volume of 20.0  $\mu$ L. The PCR thermal program was set at 95 °C for 3.0 min; then 27 cycles were conducted at 95, 55, and 72 °C for 30.0, 30.0, and 45.0 s respectively. Lastly, a final extension was conducted at 72 °C for 10.0 min.

The Quantitative Insights Into Microbial Ecology (QIIME) software was used to process the data. The data that were shorter than 200 bp and had a quality score below 25 were removed. Ten unique barcodes were used to accurately allocate the sequences of each sample and only the sequences with identity above 97% were divided for operational taxonomic unit (OTU) analysis. The most abundant sequence was defined as the representative sequence and was assigned by python Nearest Alignment Space Termination (PyNASt), then employed for clarification of the taxonomy according to the Greengenes database.

## 3. Results and discussion

### 3.1. Enhanced removal of oxytetracycline by synergistic degradation

For the static test, the concentration change protocols for different mechanisms during short-term experiments (10 h) are shown in Fig. 1a. Light excitation of photoelectrons coupled with bio-photocatalysis was used as a synergistic degradation method. In addition, the influence of absorption, photolysis, biodegradation, and photocatalytic degradation of oxytetracycline had to be taken into consideration.

For the absorption performance, the final removal rates of the

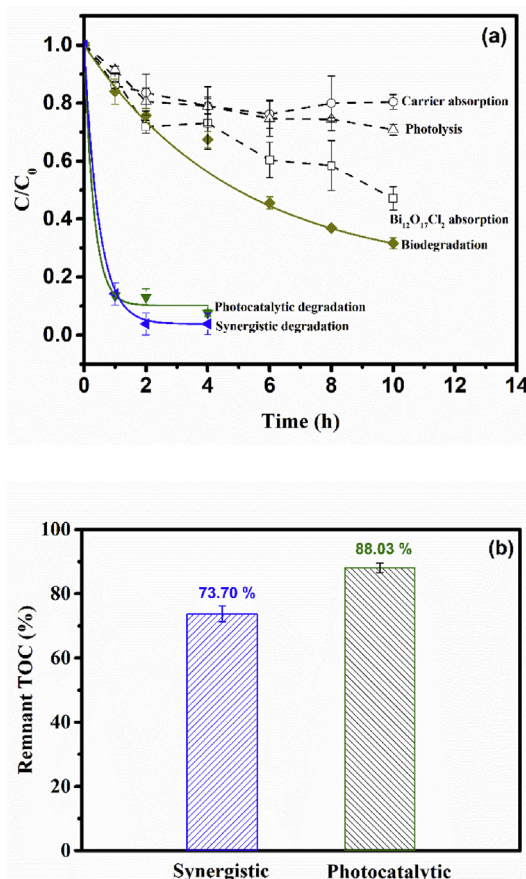


**Fig. 1.** (a) Reduction of oxytetracycline under different operating conditions: Lines of biodegradation, photocatalytic degradation, and the synergistic degradation were fitted to  $C = C_0 e^{-kt}$ . The respective oxytetracycline removal rate ( $k$ ) and half-life time ( $t_{1/2}$ ) were biodegradation:  $R^2 = 0.9746$ ,  $k = 0.1176 \pm 0.0521$ ,  $t_{1/2} = 5.8929$  h; photocatalytic degradation:  $R^2 = 0.9927$ ,  $k = 3.2118 \pm 1.3150$ ,  $t_{1/2} = 0.2158$  h; synergistic degradation:  $R^2 = 0.9996$ ,  $k = 2.1941 \pm 0.1030$ ,  $t_{1/2} = 0.3158$  h, (b) The remnant TOC after photocatalytic degradation and the synergistic degradation operation after 10 h. The initial oxytetracycline concentration for each experiment was 10.0 mg/L.

polyurethane carriers and  $\text{Bi}_{12}\text{O}_{17}\text{Cl}_2$  were  $19.55 \pm 2.53$  and  $52.86 \pm 4.07\%$ , respectively. Otherwise, oxytetracycline was rather stable under visible light irradiation as the final removal rate of the photolytic process was  $29.15 \pm 1.84\%$ . In addition, oxytetracycline proved to be significantly refractory and bio-recalcitrant. The bio-removal rate was  $68.39 \pm 1.94\%$  after 10 h, even though the microbes had been cultivated in 10.0 mg/L oxytetracycline for one year. Thus, we concluded that oxytetracycline could not be efficiently degraded in the natural environment.

Combining the photocatalysis function significantly increased the removal rates for the photocatalysis and synergistic degradation of oxytetracycline. Due to the detection limit of the instrument, the remnant oxytetracycline after photocatalysis and the synergistic degradation could not be detected after 4 h, when the final removal rates were  $92.39 \pm 2.51$  and  $96.16 \pm 3.63\%$  respectively. Fitting these results to the first order reaction model further confirmed the rapid removal rate of oxytetracycline using photocatalysis and the synergetic system. The rate constants,  $k$ , for the photocatalytic and synergistic degradation were 27.3 and 18.7 times higher, respectively, than that of biodegradation alone, revealing the much more efficient removal of oxytetracycline through photocatalysis using  $\text{Bi}_{12}\text{O}_{17}\text{Cl}_2$  during the short-term experiment.

For further investigating the superior degradation performance of the synergetic degradation system, we tested the remnant TOC from photocatalysis and the synergetic system. As shown in Fig. 1b, a nearly additional 14.3% removal rate of TOC was obtained using the synergetic degradation function compared to photocatalytic degradation alone. Notably, the extra removal of TOC should be attributed to the combined microbial system, revealing the maintaining of microbial activity in the synergetic system and the advantage of the synergetic degradation function. Three-dimensional fluorescence spectra (Fig. S4) tests also revealed that

both photocatalytic and microbial degradation occurred during the synergetic degradation process. Moreover, the results revealed that, for the short-time experiment conducted without protecting the microbes inside the carrier, the light-excited photoelectrons coupled with the bio-photocatalytic degradation system performed well in the modified carrier.

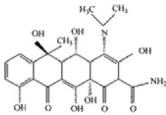
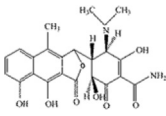
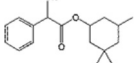
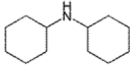
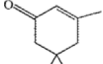
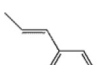
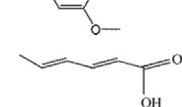
### 3.2. Degradation intermediates of oxytetracycline by synergistic degradation

The highlighted byproducts generated during the short-term experiment by the synergistic degradation system were explored using mass spectrometry. The retention times, formulas, and proposed structures of the products are presented in Table 1. The evolution of each byproduct is displayed in Fig. 2a, and the spectra of the extracted ions are illustrated in Fig. S5.

Seven compounds with different molecular weights were identified using the positive ionization mode of the mass spectrometer, within the 100–1000 m/z range (Table 1). The m/z of 461.1545, which corresponded oxytetracycline, was reduced dramatically within 2.5 h (Fig. 2a). This was consistent with the results in Fig. 1a. The detected byproducts were formed within 10 min (Fig. 2a), accumulated prior to 60 min and showed dramatic reduction in concentrations thereafter. However, only one of the six identified intermediates,  $\beta$ -apo-oxytetracycline, which had an m/z of 443.4102, has been previously reported as a degradation product of oxytetracycline. Thus, we evaluated the toxicities of the identified intermediates.

$\beta$ -apo-oxytetracycline (m/z of 443.4102), one of the main antimicrobial active degradation products of oxytetracycline, was reported to be quite stable, exhibiting a half-life of 270 d in soil interstitial water (Halling-Sørensen et al., 2003). Moreover,  $\beta$ -apo-oxytetracycline was found in animal tissue, agricultural products,

**Table 1**  
Detected mass-to-charge ratios, retention times, proposed formulas, molecular weights, and structures of effluent samples.

Retention time	Ionization mode	m/z	Proposed formula	Molecular weight	Proposed structure
6.321	ESI+	461.1545	$\text{C}_{22}\text{H}_{24}\text{N}_2\text{O}_9$	460.1482	
9.257	ESI+	443.4102	$\text{C}_{22}\text{H}_{22}\text{N}_2\text{O}_8$	442.4200	
10.202	ESI+	277.1789	$\text{C}_{17}\text{H}_{24}\text{O}_3$	276.1726	
7.790	ESI+	182.1889	$\text{C}_{12}\text{H}_{23}\text{N}$	181.1830	
9.141	ESI+	139.1114	$\text{C}_9\text{H}_{14}\text{O}$	138.1041	
10.016	ESI+	149.0957	$\text{C}_{10}\text{H}_{12}\text{O}$	148.0888	
9.781	ESI+	113.0596	$\text{C}_6\text{H}_8\text{O}_2$	112.0524	

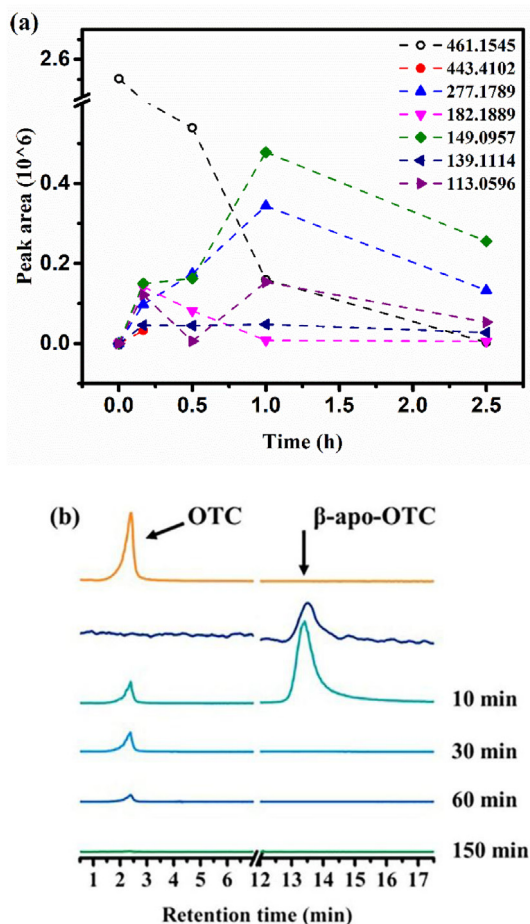


**Fig. 2.** (a) Evolution of oxytetracycline and the main degradation byproducts by the performance of the synergistic degradation in the initial and 10, 30, 60 and 150 min. The extracted mass-to-charge ratio ranged from 100 to 1000, (b) UPLC-MS spectra of the degradation effluent by fitting to the oxytetracycline and  $\beta$ -apo-oxytetracycline standards.

and dosage forms (Loke et al., 2003). In the synergistic degradation process,  $\beta$ -apo-oxytetracycline was detected at 10 min and without further accumulation. This observation was also confirmed using the  $\beta$ -apo-oxytetracycline standard employing an analytical method previously reported in the literature (Halling-Sørensen et al., 2003) (Fig. 2b). Apparently,  $\beta$ -apo-oxytetracycline is harmful and difficult to be decomposed in the natural environment. Its quick decomposition by the photoelectron coupled bio-photocatalytic degradation system should contribute to the synergistic performance. Cyclandelate (m/z of 277.1789) plays an important role in the treatment of hemorrhological disorders and thrombosis (Diener et al., 1996). Dicyclohexylamine (m/z of 182.1889) has always been detected in hive products (Heever et al., 2014). Although chronic exposure to isophorone (m/z of 139.1114) could increase the possibility of developing dizziness or depression, photooxidation could efficiently remove isophorone and thus reduced its negative effects on the environment (Borup and Middlebrooks, 1987; Wei et al., 2013). Thus, low dose isophorone (Fig. 2a) could be easily removed using the synthetic degradation procedure. The product with m/z of 149.0957, which may be trans-anethole, was reported to undergo efficient metabolic detoxication and did not present any significant risk to human health (Newberne et al., 1999). In addition, sorbic acid (m/z of 113.0596) was rapidly metabolized and did not exhibit carcinogenic activity (Walker, 1990).

Food safety and human health concerns should never be ignored. However, negative consequences always involve long-term exposure and high-enough dosage of harmful agents. The evolution of the main intermediates of the synergistic oxytetracycline degradation illustrated an efficient removal of these compounds without any accumulation after 60 min of operation, indicating the enhanced degradation of oxytetracycline and the decomposition of the subsequent intermediates. Compared with previous works that analyzed the degradation of oxytetracycline (Halling-Sørensen et al., 2003; Liu et al., 2016), the degradation reaction using the synergetic degradation system was more efficient.

### 3.3. Degradation stability of oxytetracycline by synergistic degradation

As the degradation process progressed, it was observed that the efficiency of the degradation gradually declined because of biofilms detachment and the decrease in catalytic activity of photocatalysts. To measure the stability of this type of photoelectron coupled bio-photocatalytic system for degrading oxytetracycline, the continuous biodegradation, photocatalytic and the synergetic degradation with a hydraulic retention time (HRT) of 4.0 h was tested for 400 h (Fig. 3).

After adjusting for the first few hours, the removal rate of oxytetracycline by only the biodegradation process gradually increased. This should be attributed to the function of the microbial metabolism and absorption ability of the formed biofilm. However, the removal rate dramatically reduced after 228 h of operation, due to the detachment of biofilms and desorption of oxytetracycline. The photocatalytic degradation process showed excellent elimination capability for oxytetracycline. Moreover, no significant differences could be observed between the process and the synergistic degradation process over a long period of time. However, the photocatalytic degradation rate started to decrease after 156 h, and the final rate was only ~67%. This was probably due to the decrease in the catalytic activity of the photocatalysts after prolonged illumination and operation. Unlike the performance of biodegradation or photocatalysis, the efficiency of the synergetic degradation process remained above ~94% for the entire experimental period, indicating that the photoelectron coupled bio-photocatalytic degradation system could maintain good degradation stability and acclimate to the moving environment. This finding also illustrated that, even for tests conducted over long periods of time, the

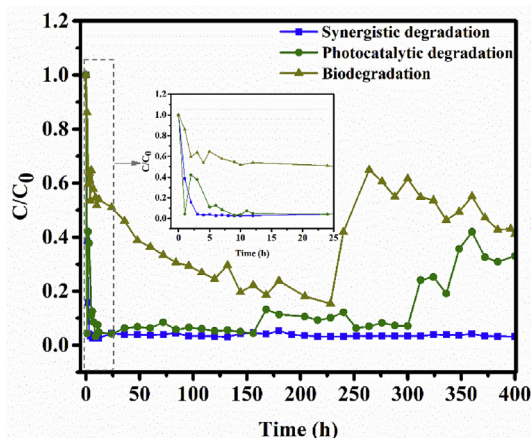


**Fig. 3.** Biodegradation, photocatalytic and the synergistic degradation in the dynamic system with a hydraulic retention time of 4.0 h. The initial oxytetracycline concentration was 10.0 mg/L, and the ambient temperature was  $22 \pm 2$  °C.

coated microbes of the synergistic system was not apoptosis, and microbial activity was well maintained.

In addition, the biotoxicity of the effluent after 400 h of synergistic degradation was investigated by inoculating *Escherichia coli* DH5 $\alpha$  using the effluent (Fig. S6). The inhibitory effect of oxytetracycline was obvious compared with the milli Q group. However, after the synergistic degradation treatment, the biotoxicity and antibacterial activity of the effluent were dramatically reduced. According to our results, the synergetic degradation protocol not only exhibited a high degradation rate for oxytetracycline but also maintained the ability to decompose its intermediates.

### 3.4. Photo-electrochemical measurements

As mentioned above, the synergetic degradation procedure could not simply be separated into biodegradation and photocatalytic degradation. Adequate exposure to visible light induced the transfer of photoelectrons between the two attached parts, and this was utilized for environmental remediation (Jiang et al., 2014; Li et al., 2014). The existing connections between the photocatalyst and microbes may provide the potential for synergistic energy conversion and contribute to the enhanced degradation of oxytetracycline. As evidence, photo-electrochemical tests were performed to illustrate the interplay electron transfer between Bi<sub>12</sub>O<sub>17</sub>Cl<sub>2</sub> and microbes under visible light irradiation. During electrochemical tests, blank and coated stainless-steel meshes were utilized as photo-anodes because the wire ingredient and net structure of the stainless-steel mesh were analogous to the sponge carrier. The good conductivity of the mesh also ensured the timely collection of electrons.

In Fig. 4a, a photocurrent was immediately induced after the illumination of Bi<sub>12</sub>O<sub>17</sub>Cl<sub>2</sub> using visible light and no bias, because the electrons were excited into the conduction band and holes (positive charges) were generated in the valence band. When the illumination was stopped, the photocurrent declined, indicating that Bi<sub>12</sub>O<sub>17</sub>Cl<sub>2</sub> acted as photocatalyst and the transport of photoelectrons was fast. Theoretically, when the electrode was coated with microbes, the obtained photocurrent would be reduced, because light would be obstructed from reaching the photocatalysts, and microbes would be insensitive to light irradiation. However, when the electrode was coated with microbes, the photocurrent did not decline, the photocatalytic activity maintained, revealing an additional electron transfer pathway in the synergetic system.

In addition, photoelectrochemical impedance spectroscopy analysis and linear sweep voltammetry were further used to expand the electron transmission at the interface between Bi<sub>12</sub>O<sub>17</sub>Cl<sub>2</sub> and microbes. The improved conductivity of the synergetic system compared to the photocatalyst alone was evidenced by the EIS results (Fig. 4b). It was obvious that the synergetic system showed a smaller circle in both the low and high frequency regions than the photocatalytic system alone. Hence, the synergetic interface was more conducive to electron transmission than the photocatalyst. Without bias, the decrease in circles was small after the light irradiation.

Linear sweep voltammetry within the 0.45–0.85 V potential range (versus Ag/AgCl, KCl (sat'd)) was used to represent the effect of different potentials on photocurrent promotion (Fig. 4c). The stainless-steel mesh was electrochemically stable in this potential range, and most of the bio-electrochemical signal could be excluded. The current of the synergetic system was higher than of the photocatalytic system in the dark, which was consistent with the EIS test results. Under visible light illumination, the photocurrent gradually increased. The photoinduced current reached 52.1 and 39.9  $\mu\text{A}/\text{cm}^2$  for the synergetic and photocatalytic systems,

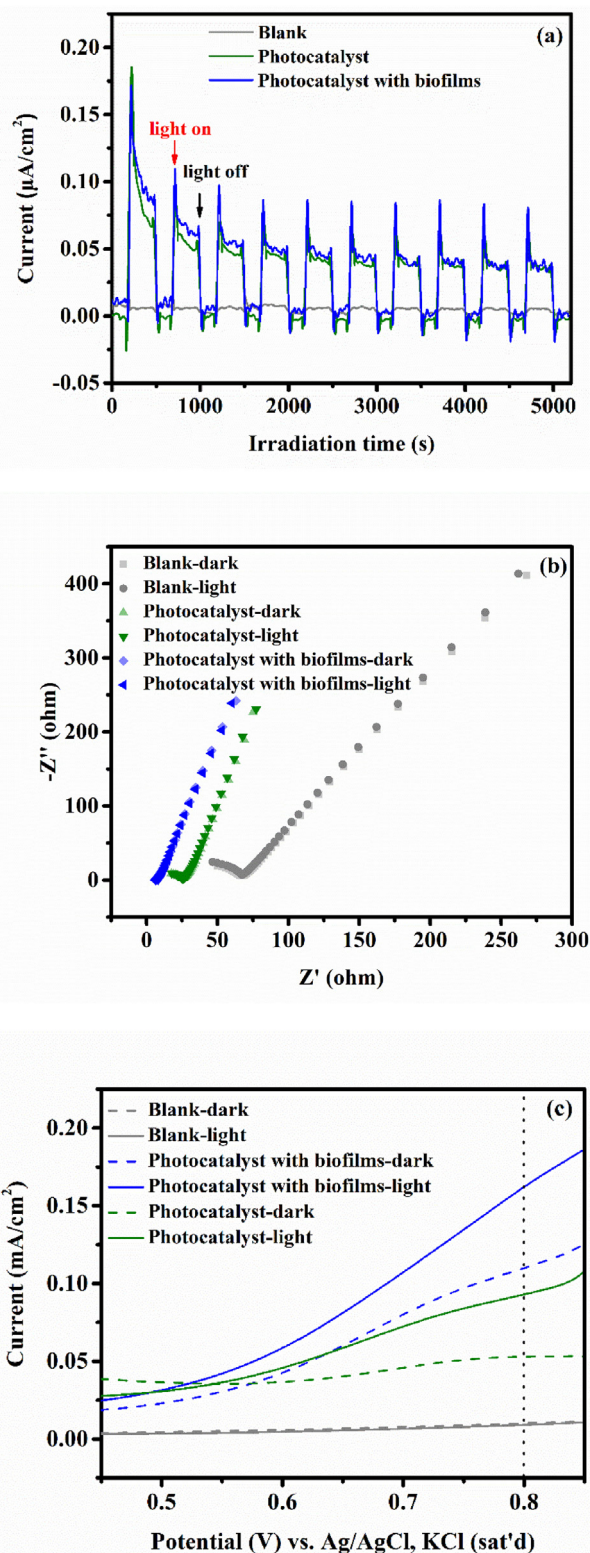


**Fig. 4.** Photo-electrochemical characterization of photocatalytic and synergistic system: (a) Amperometric I-t curves applied with no bias; the illumination cycle was 300 s irradiation and 200 s dark, (b) Photo-electrochemical impedance spectroscopy of each tests with no bias; the frequency was changed from 200 kHz to 10 Hz with an amplitude of 10 mV, (c) Linear scan voltammogram tests ranged from 0.45 to 0.85 V at a scanning rate of 10 mV/s.

respectively, at 0.8 V. The extra photocurrent should be attributed to the transfer of photoelectrons between  $\text{Bi}_{12}\text{O}_{17}\text{Cl}_2$  and the microbes. This implied that the synergistic system could generate more electrons for transfer than the photocatalytic system alone, which confirmed the existence of a transfer of photoelectrons between the microbes and  $\text{Bi}_{12}\text{O}_{17}\text{Cl}_2$  in the presence of light.

### 3.5. Coated microbes and functionalized microbial community

The carriers were collected. Some were coated only with  $\text{Bi}_{12}\text{O}_{17}\text{Cl}_2$  and some underwent synergetic degradation for 400 h. As shown in Fig. 5, compared to the blank carrier (Fig. 5a and b), the surface of each carrier fiber become rough after coating with  $\text{Bi}_{12}\text{O}_{17}\text{Cl}_2$  (Fig. 5c and d). After the microbe culture, the porosity of the carrier decreased and microorganisms attached tightly to  $\text{Bi}_{12}\text{O}_{17}\text{Cl}_2$  (Fig. 5e and f). Instead of forming a condensed biofilm, microbes were dispersed. Three reasons might contribute to this phenomenon. First, without the protection of the carrier, direct exposure to toxicants and oxidants would exert negative effects on the formation of biofilms. Second, the light-excited photoelectrons, however, could be harvested by microbes to stimulate their growth and modulate the microbial community to acclimate to the surrounding environment. Third, the big porosity of the carrier provided channels for the easy transmission of substrates, and the free radicals could undergo immediate degradation, thus their negative influence on the microbes could be weakened.

The microbial community transformation analysis revealed that the bacterial community was regulated after a long degradation process (Fig. S7). Except for the original three classes of Gram-proteobacteria, Bacilli, and Flavobacteria, five additional classes flourished: Beta-proteobacteria, Alpha-proteobacteria, Clostridia, Sphingobacteria, and Actinobacteria.

The heat map (Fig. 6) clearly displayed the evolution of the microbial community at the genus level. *Rhodopseudomonas*, which was both phototrophic and chemotrophic, emerged after the degradation process (Larimer et al., 2004), indicating an adaption to the synergetic environment. *Rhodopseudomonas* (Martin et al., 1986), *Lysinibacillus* (Nandy et al., 2013), *Sphingobacterium*, *Pseudomonas*, *Burkholderia*, *Escherichia*, and *Bacillus*, which were much abundant, have the ability of extracellular transfer electrons (Huang et al., 2011), revealing the potential for the transfer of photoelectrons between the microbes and photocatalysts. In addition, the population of *Pseudomonas* (Kiyohara et al., 1992), *Stenotrophomonas* (Qureshi et al., 2007), *Achromobacter* (Wang et al., 2016), and *Sphingomonas* (Ye et al., 1996), which were capable of scavenging aromatic hydrocarbons were largely increased. The newly emerged *Mycobacterium* (Schneider et al., 1996), *Comamonas* (Goyal and Zylstra, 1996), *Lysinibacillus* (Atefeh et al., 2013), *Dokdonella* (Bacosa and Inoue, 2015), *Sulfobacillus* (Zhou et al., 2016), *Bacillus* (Arutchelvan et al., 2006), *Pandoraea* (Wang et al., 2015), and *Ochrobactrum* (Ghosal et al., 2010) genera were also able to degrade aromatic hydrocarbons. Moreover,

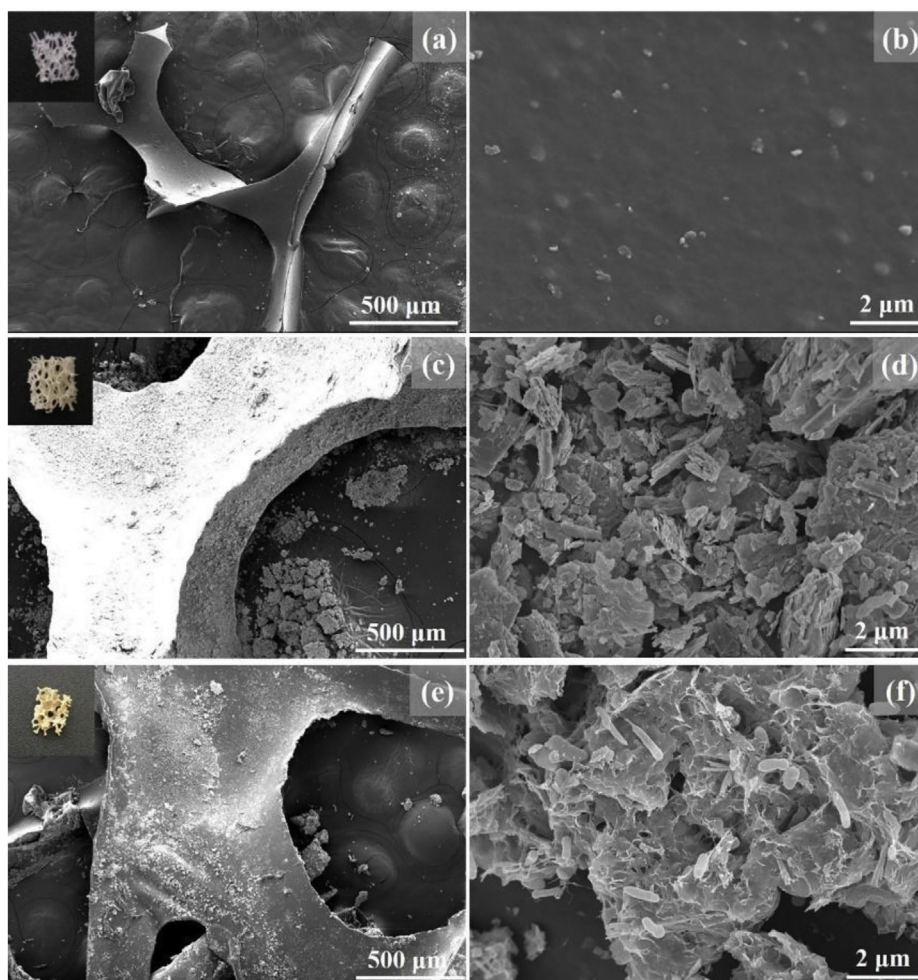


Fig. 5. SEM images of the blank sponge carrier (a, b), coated with  $\text{Bi}_{12}\text{O}_{17}\text{Cl}_2$  (c, d) and after the synergistic degradation operation for 400 h (e, f).

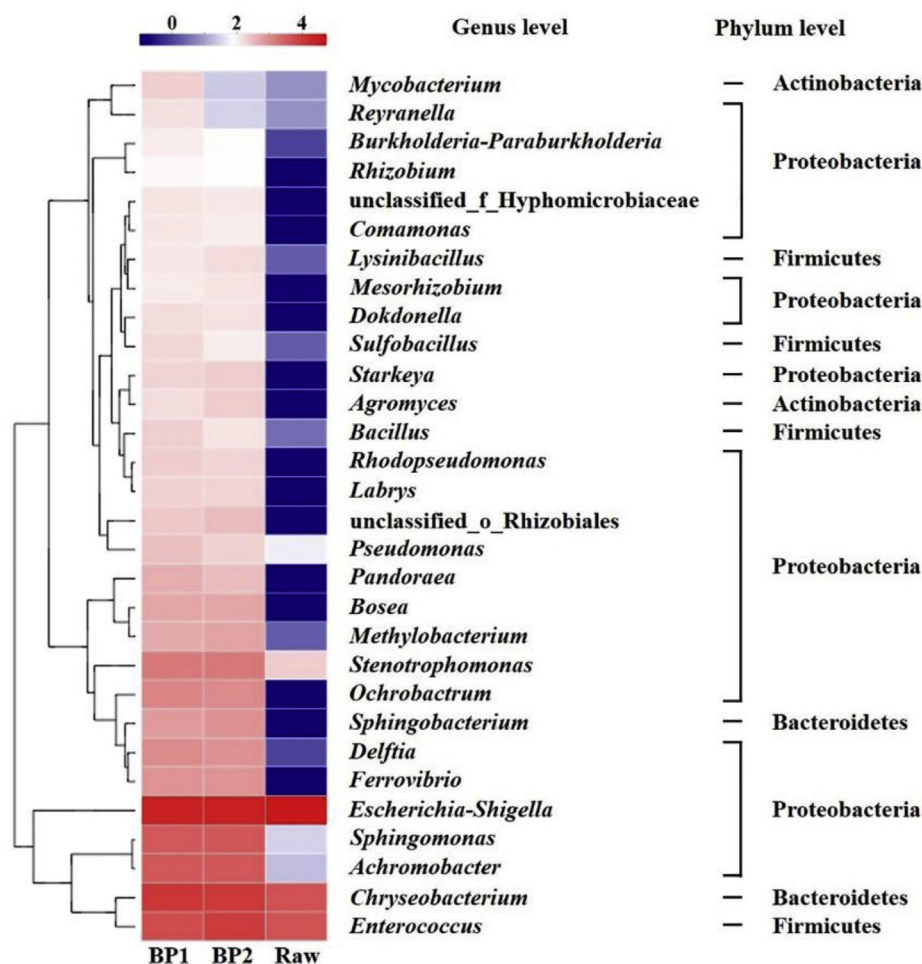


Fig. 6. Pyrosequencing results of DNA from the microbial community before (Raw) and after (BP) the synergetic degradation at the genus and phylum levels.

*Mesorhizobium* (Okada et al., 2005) and *Methylobacterium* (Jourand et al., 2004) contributed to the denitrification process, while *Labrys* (Amorim et al., 2014) and *Sphingobacterium* (Ghosh et al., 2009) were reported to degrade antibiotics. The flourishing of these microorganisms expounded the formation of functional microbial groups for the degradation of oxytetracycline and mineralization of byproducts.

The results also validated the feasibility of the design protocol in this study. Given a suitable porosity of carrier, the microbes need not be cultivated just inside carriers for protection purposes. The energy source generated by the light-excited photoelectrons could be used by microbes to reconstruct their microbial communities to adapt to the environment.

#### 4. Conclusions

In this study, a simple protocol was developed to enhance the bio-photocatalytic degradation efficiency of oxytetracycline by stimulating the transfer of photoelectrons between the photocatalysts and microbes using a higher porosity carrier (95%). The protocol did not involve the additional of supplementary electron donors for microbe metabolism or improving the loading rate of the photocatalysts. Although exposure to toxicants and oxidants, the negative influence on microbes could be weakened. A removal rate of ~94% was maintained for 400 h and the lack of cytotoxic effects of

the effluent demonstrated the degradation stability of the synergetic degradation system. In addition,  $\beta$ -apo-oxytetracycline, the refractory and antimicrobial active intermediate in the degradation of oxytetracycline, could be further degraded in 10 min without accumulation. Therefore, we provide a simple and efficient strategy to enhance the degradation efficiency of the bio-photocatalytic process for oxytetracycline and confirms the potential application value of the strategy for realistic situation.

#### Acknowledgement

This work was supported by NSFC (21777155 and 41471260), the Xiamen Science and Technology Program (3502Z20172027) and the Fujian STS Project (2016T3032).

#### Appendix A. Supplementary data

Supplementary data related to this article can be found at <https://doi.org/10.1016/j.watres.2018.06.068>.

#### References

- Amorim, C.L., Moreira, I.S., Maia, A.S., Tiritan, M.E., Castro, P.M.L., 2014. Biodegradation of ofloxacin, norfloxacin, and ciprofloxacin as single and mixed substrates by *Labrys portucalensis* F11. *Appl. Microbiol. Biotechnol.* 98 (7), 3181–3190.

- Arutchelvan, V., Kanakasabai, V., Elangovan, R., Nagarajan, S., Muralikrishnan, V., 2006. Kinetics of high strength phenol degradation using *Bacillus brevis*. *J. Hazard Mater.* 129 (1), 216–222.
- Ashfaq, M., Li, Y., Wang, Y., Chen, W., Wang, H., Chen, X., Wu, W., Huang, Z., Yu, C.P., Sun, Q., 2017. Occurrence, fate, and mass balance of different classes of pharmaceuticals and personal care products in an anaerobic-anoxic-oxic wastewater treatment plant in Xiamen, China. *Water Res.* 123, 655–667.
- Atefeh, E., Ali, P.A., Ali, A.H., Farzin, S., Ensieh, E., 2013. Biodegradation of low-density polyethylene (LDPE) by mixed culture of *Lysinibacillus xylanilyticus* and *Aspergillus Niger* in Soil. *PLoS One* 8 (9), e71720.
- Bacosa, H.P., Inoue, C., 2015. Polycyclic aromatic hydrocarbons (PAHs) biodegradation potential and diversity of microbial consortia enriched from tsunami sediments in Miyagi, Japan. *J. Hazard Mater.* 283, 689–697.
- Borup, M.B., Middlebrooks, E.J., 1987. *Photocatalysed Oxidation of Toxic Organics*. Iwa Publishing.
- Chen, Q., Wu, S., Xin, Y., 2016. Synthesis of Au-CuS-TiO<sub>2</sub> nanobelts photocatalyst for efficient photocatalytic degradation of antibiotic oxytetracycline. *Chem. Eng. J.* 302, 377–387.
- Diener, H.C., Föh, M., Iaccarino, C., Wessely, P., Isler, H., Strenge, H., Fischer, M., Wedekind, W., Taneri, Z., 1996. Cyclandelate in the prophylaxis of migraine: a randomized, parallel, double-blind study in comparison with placebo and propranolol. *The Study group. Cephalalgia An Int. J. Headache* 16 (6), 441–447.
- Ding, R., Zhao, F., 2017. Intimate coupling of photocatalysis and biodegradation to synchronously degrade pollutants. *Prog. Chem.* 29 (9), 1154–1158.
- Duan, X., Fu, T.M., Liu, J., Lieber, C.M., 2013. Nanoelectronics-biology frontier: from nanoscopic probes for action potential recording in live cells to three-dimensional cyborg tissues. *Nano Today* 8 (4), 351–373.
- Ghosal, D., Chakraborty, J., Khara, P., Dutta, T.K., 2010. Degradation of phenanthrene via meta-cleavage of 2-hydroxy-1-naphthoic acid by *Ochrobactrum* sp. strain PWTJD. *FEMS (Fed. Eur. Microbiol. Soc.) Microbiol. Lett.* 313 (2), 103–110.
- Ghosh, S., Sadowsky, M.J., Roberts, M.C., Gralnick, J.A., Lapara, T.M., 2009. *Sphingobacterium* sp. strain PM2-P1-29 harbours a functional tet(X) gene encoding for the degradation of tetracycline. *J. Appl. Microbiol.* 106 (4), 1336–1342.
- Goyal, A.K., Zylstra, G.J., 1996. Molecular cloning of novel genes for polycyclic aromatic hydrocarbon degradation from *Comamonas testosteroni* GZ39. *Appl. Environ. Microbiol.* 62 (1), 230–236.
- Halling-Sørensen, B., Lykkeberg, A., Ingwerslev, F., Blackwell, P., Tjørnelund, J., 2003. Characterisation of the abiotic degradation pathways of oxytetracyclines in soil interstitial water using LC-MS-MS. *Chemosphere* 50 (10), 1331–1342.
- Heever, J.P.V.D., Thompson, T.S., Curtis, J.M., Ibrahim, A., Pernal, S.F., 2014. Fumagillin: an overview of recent scientific advances and their significance for apiculture. *J. Agric. Food Chem.* 62 (13), 2728–2737.
- Huang, L., Regan, J.M., Quan, X., 2011. Electron transfer mechanisms, new applications, and performance of biocathode microbial fuel cells. *Bioresour. Technol.* 102 (1), 316–323.
- Jiang, X., Hu, J., Lieber, A.M., Jackan, C.S., Biffinger, J.C., Fitzgerald, L.A., Ringeisen, B.R., Lieber, C.M., 2014. Nanoparticle facilitated extracellular electron transfer in microbial fuel cells. *Nano Lett.* 14 (11), 6737–6742.
- Jourand, P., Giraud, E., Béna, G., Sy, A., Willems, A., Gillis, M., Dreyfus, B., De, L.P., 2004. *Methylobacterium nodulosum* sp. nov., for a group of aerobic, facultatively methylotrophic, legume root-nodule-forming and nitrogen-fixing bacteria. *Int. J. Syst. Evol. Microbiol.* 54 (6), 2269–2273.
- Kiyohara, H., Hatta, T., Ogawa, Y., Kakuda, T., Yokoyama, H., Takizawa, N., 1992. Isolation of *Pseudomonas pickettii* strains that degrade 2,4,6-trichlorophenol and their dechlorination of chlorophenols. *Appl. Environ. Microbiol.* 58 (4), 1276–1283.
- Larimer, F.W., Chain, P., Hauser, L., Lamerdin, J., Malfatti, S., Long, D., Land, M.L., Pelletier, D.A., Beatty, J.T., Lang, A.S., 2004. Complete genome sequence of the metabolically versatile photosynthetic bacterium *Rhodospseudomonas palustris*. *Nat. Biotechnol.* 22 (1), 55–61.
- Li, S.Z., Li, X.Y., Wang, D.Z., 2004. Membrane (RO-UF) filtration for antibiotic wastewater treatment and recovery of antibiotics. *Separ. Purif. Technol.* 34 (1–3), 109–114.
- Li, G., Park, S., Kang, D.-W., Krajmalnik-Brown, R., Rittmann, B.E., 2011. 2, 4, 5-Trichlorophenol degradation using a novel TiO<sub>2</sub>-coated biofilm Carrier: roles of adsorption, photocatalysis, and biodegradation. *Environ. Sci. Technol.* 45 (19), 8359–8367.
- Li, G., Park, S., Rittmann, B.E., 2012a. Developing an efficient TiO<sub>2</sub>-coated biofilm Carrier for intimate coupling of photocatalysis and biodegradation. *Water Res.* 46 (19), 6489–6496.
- Li, G., Park, S., Rittmann, B.E., 2012b. Degradation of reactive dyes in a photocatalytic circulating-bed biofilm reactor. *Biotechnol. Bioeng.* 109 (4), 884–893.
- Li, D.B., Cheng, Y.Y., Li, L.L., Li, W.W., Huang, Y.X., Pei, D.N., Tong, Z.H., Mu, Y., Yu, H.Q., 2014. Light-driven microbial dissimilatory electron transfer to hematite. *Phys. Chem. Chem. Phys.* 16 (42), 23003–23011.
- Liang, B., Cheng, H.Y., Kong, D.Y., Gao, S.H., Sun, F., Cui, D., Kong, F.Y., Zhou, A.J., Liu, W.Z., Ren, N.Q., 2013. Accelerated reduction of chlorinated nitroaromatic antibiotic chloramphenicol by biocathode. *Environ. Sci. Technol.* 47 (10), 5353–5361.
- Liu, Y., He, X., Duan, X., Fu, Y., Fatta-Kassinos, D., Dionysiou, D.D., 2016. Significant role of UV and carbonate radical on the degradation of oxytetracycline in UV-AOPs: kinetics and mechanism. *Water Res.* 95, 195–204.
- Loke, M.L., Jespersen, S., Vreeken, R., Halling-Sørensen, B., Tjørnelund, J., 2003. Determination of oxytetracycline and its degradation products by high-performance liquid chromatography-tandem mass spectrometry in manure-containing anaerobic test systems. *J. Chromatogr. B Anal. Technol. Biomed. Life Sci.* 783 (1), 11–23.
- Lovley, D.R., 2011. Live wires: direct extracellular electron exchange for bioenergy and the bioremediation of energy-related contamination. *Energy Environ. Sci.* 4 (12), 4896–4906.
- Lu, A., Li, Y., Jin, S., Wang, X., Wu, X.L., Zeng, C., Li, Y., Ding, H., Hao, R., Lv, M., 2012. Growth of non-phototrophic microorganisms using solar energy through mineral photocatalysis. *Nat. Commun.* 3 (1), 768.
- Marsolek, M.D., Torres, C.I., Hausner, M., Rittmann, B.E., 2008. Intimate coupling of photocatalysis and biodegradation in a photocatalytic circulating-bed biofilm reactor. *Biotechnol. Bioeng.* 101 (1), 83–92.
- Martin, J.L., Breton, J., Hoff, A.J., Migus, A., Antonetti, A., 1986. Femtosecond spectroscopy of electron transfer in the reaction center of the photosynthetic bacterium *Rhodospseudomonas sphaeroides* R-26: direct electron transfer from the dimeric bacteriochlorophyll primary donor to the bacteriopheophytin acceptor with a Ti. *Proc. Natl. Acad. Sci. U.S.A.* 83 (4), 957–961.
- Nandy, A., Kumar, V., Kundu, P.P., 2013. Utilization of proteinaceous materials for power generation in a mediatorless microbial fuel cell by a new electrogenic bacteria *Lysinibacillus sphaericus* VA5. *Enzym. Microb. Technol.* 53 (5), 339–344.
- Newberne, P., Smith, R.L., Doull, J., Goodman, J.J., Munro, I.C., Portoghese, P.S., Wagner, B.M., Weil, C.S., Woods, L.A., Adams, T.B., 1999. The FEMA GRAS assessment of trans-anethole used as a flavouring substance. *Flavour and Extract Manufacturer's Association. Food Chem. Toxicol.* 37 (7), 789–811.
- Okada, N., Nomura, N., Kambe, T., Uchiyama, H., 2005. Characterization of the aerobic denitrification in *Mesorhizobium* sp. Strain NH14 in comparison with that in related *Rhizobia*. *Microb. Environ.* 20 (4), 208–215.
- Pereira, J.H.O.S., Queirós, D.B., Reis, A.C., Nunes, O.C., Borges, M.T., Rui, A.R.B., Vilar, V.J.P., 2014. Process enhancement at near neutral pH of a homogeneous photo-Fenton reaction using ferric-carboxylate complexes: application to oxytetracycline degradation. *Chem. Eng. J.* 253 (2), 217–228.
- Qureshi, A., Verma, V., Kapley, A., Purohit, H.J., 2007. Degradation of 4-nitroaniline by *Stenotrophomonas* strain HPC 135. *Int. Biodeterior. Biodegrad.* 60 (4), 215–218.
- Rittmann, B.E., 2017. Biofilms, active substrata, and me. *Water Res.* 132, 135–145.
- Sakimoto, K.K., Wong, A.B., Yang, P., 2016. Self-photosensitization of non-photosynthetic bacteria for solar-to-chemical production. *Science* 351 (6268), 74–77.
- Schneider, J., Grosser, R., Jayasimhulu, K., Xue, W., Warshawsky, D., 1996. Degradation of pyrene, benz[a]anthracene, and benzo[a]pyrene by *Mycobacterium* sp. strain RJGII-135, isolated from a former coal gasification site. *Appl. Environ. Microbiol.* 62 (1), 13–19.
- Vaz, S., Lopes, W.T., Martin-Neto, L., 2015. Study of molecular interactions between humic acid from Brazilian soil and the antibiotic oxytetracycline. *Environ. Technol. Innovat.* 4, 260–267.
- Walker, R., 1990. Toxicology of sorbic acid and sorbates. *Food Addit. Contam.* 7 (5), 671–676.
- Wang, X., Wang, Q., Li, S., Wei, L., 2015. Degradation pathway and kinetic analysis for pyrene removal by a novel *Pandoraea* sp. strain WL1 and its application in a biotrickling filter. *J. Hazard Mater.* 288, 17–24.
- Wang, L., Liu, Y., Ma, J., Zhao, F., 2016. Rapid degradation of sulphamethoxazole and the further transformation of 3-amino-5-methylisoxazole in a microbial fuel cell. *Water Res.* 88, 322–328.
- Wang, C.Y., Zhang, X., Qiu, H.B., Wang, W.K., Huang, G.X., Jiang, J., Yu, H.Q., 2017. Photocatalytic degradation of bisphenol A by oxygen-rich and highly visible-light responsive Bi<sub>12</sub>O<sub>17</sub>Cl<sub>2</sub> nanobelts. *Appl. Catal. B Environ.* 200, 659–665.
- Wei, H., Yan, X., Li, X., He, S., Sun, C., 2013. The degradation of isophorone by catalytic wet air oxidation on Ru/TiZrO<sub>4</sub>. *J. Hazard Mater.* 244–245, 478–488.
- Wen, D., Li, G., Xing, R., Park, S., Rittmann, B.E., 2012. 2, 4-DNT removal in intimately coupled photobiocatalysis: the roles of adsorption, photolysis, photocatalysis, and biotransformation. *Appl. Microbiol. Biotechnol.* 95 (1), 263–272.
- Xiong, H., Zou, D., Zhou, D., Dong, S., Wang, J., Rittmann, B.E., 2017. Enhancing degradation and mineralization of tetracycline using intimately coupled photocatalysis and biodegradation (ICPB). *Chem. Eng. J.* 316, 7–14.
- Xiong, H., Dong, S., Zhang, J., Zhou, D., Rittmann, B.E., 2018. Roles of an easily biodegradable co-substrate in enhancing tetracycline treatment in an intimately coupled photocatalytic-biological reactor. *Water Res.* 136, 75–83.
- Yan, W., Guo, Y., Xiao, Y., Wang, S., Ding, R., Jiang, J., Gang, H., Wang, H., Yang, J., Zhao, F., 2018. The changes of bacterial communities and antibiotic resistance genes in microbial fuel cells during long-term oxytetracycline processing. *Water Res.* 142, 105–114.
- Ye D, Siddiqi, M.A., Maccubbin, A.E., Kumar, S., Sikka, H.C., 1996. Degradation of polynuclear aromatic hydrocarbons by *Sphingomonas paucimobilis*. *Environ. Sci. Technol.* 30 (1), 136–142.
- Zhang, L., Xing, Z., Zhang, H., Li, Z., Wu, X., Zhang, X., Zhang, Y., Zhou, W., 2016. High thermostable ordered mesoporous SiO<sub>2</sub>-TiO<sub>2</sub> coated circulating-bed biofilm reactor for unpredictable photocatalytic and biocatalytic performance. *Appl. Catal. B Environ.* 180, 521–529.
- Zhao, C., Pelaez, M., Duan, X., Deng, H., O'Shea, K., Fatta-Kassinos, D., Dionysiou, D.D., 2013. Role of pH on photolytic and photocatalytic degradation

- of antibiotic oxytetracycline in aqueous solution under visible/solar light: kinetics and mechanism studies. *Appl. Catal. B Environ.* 134–135 (5), 83–92.
- Zhou, D., Xu, Z., Dong, S., Huo, M., Dong, S., Tian, X., Cui, B., Xiong, H., Li, T., Ma, D., 2015. Intimate coupling of photocatalysis and biodegradation for degrading phenol using different light types: visible light vs UV light. *Environ. Sci. Technol.* 49 (13), 7776–7783.
- Zhou, W., Guo, W., Zhou, H., Chen, X., 2016. Phenol degradation by *Sulfobacillus acidophilus* TPY via the meta-pathway. *Microbiol. Res.* 190, 37–45.
- Zhou, D., Dong, S., Shi, J., Cui, X., Ki, D., Torres, C.I., Rittmann, B.E., 2017. Intimate coupling of an N-doped TiO<sub>2</sub> photocatalyst and anode respiring bacteria for enhancing 4-chlorophenol degradation and current generation. *Chem. Eng. J.* 317, 882–889.